AL41 - Artificial Neural Networks for Predicting and Improving HF Generation and Recovery Efficiency

Joseph Ndjebayi Nloga[1], Herman Vermette[2], Jonathan Bernier[3] and Jean-Nicolas Maltais[4]

1. Principal Advisor Technical Services Rio Tinto Atlantic
2. Technical Manager Reduction, Technical Services Rio Tinto Atlantic
3. Principal Adviser R&D Environment and Climate Change Solutions Technologiques Aluminium – Arvida Research and Development Centre
4. Principal Advisor Gas Collection and Treatment – Technical services

Corresponding author: jose.ndjebayinloga@riotinto.com

Abstract

Brownfield aluminum plants have increasingly focused on controlling hydrogen fluoride (HF) emissions due to amperage increase, which can lead to higher gas temperature and HF generation. Increase in HF emissions can restrict strategic initiatives such as amperage increase unless smelters generate significant investment to boost the gas treatment center (GTC) capacity. Previous research has focused on the hooding and scrubbing efficiencies to reduce HF emissions. Other more recent investigations have produced models to estimate the HF generation following feeding periods, and depending on the relative air humidity, as well as the loss on ignition (LOI) (volatile hydrous) in alumina. However, none of these models yields concrete operational applications for decision makers in allowing the quantification of HF emissions during each of the main operational activities. Thus, the models do not incorporate structural, systemic, or operational factors into the quantification of individual sources of hydrogen fluoride emissions. In a modern Rio Tinto smelter, supervised machine learning (SML), comprising artificial neural networks (ANN), was used to analyze the factors and the distribution of HF emissions in a multifactorial modeling problem. The model uses a multi-dimensional dataset and can predict, with over 90 % accuracy, the influence of systemic, structural, and operational factors on HF emissions. These factors can hinder amperage increase. The results showed that the most effective way to improve HF recovery is to scale down generation by operational strategies and process parameter settings. This research contributes to business practices by providing a statistical capability for predicting and planning HF emissions according to draft/kA ratio, seasonality, process settings, systemic factors (work delays), operational excellence, and structural factors (e.g., anode geometry, gas kinetics, temperature, etc.).

Key words: Gas kinetics, HF generation and emissions, HF emissions planning, Artificial neural networks, Statistical modeling.

1. Introduction

Primary aluminum smelting can generate significant HF emissions. One of the most important responsibilities of the aluminum manufacturers is to protect worker safety, ambient air, water, and soil. Companies must measure HF concentrations in smelters at multiple locations through gas treatment center (GTC) stack sampling or continuous emission monitoring (CEM) at roof vents. The gas treatment centers then play a crucial role in cutting down HF emissions through internal recycling via adsorption on smelter grade alumina. Production-rate increase requires brown field smelters to improve their processing capacity, including GTC capacity, standard work methods, and process control. Adding more stress to resources operating at full capacity can have harmful effects. According to research, GTC gas recovery performance can suffer if gas temperature rises due to increased potline amperage and internal heat [1]. CEM device alone cannot prevent HF emissions generation, even though it can detect abnormalities. Smelters need a more compelling and proactive approach in providing robustness against high HF generation.

In most countries, governments are actively protecting workers safety and environmental receptors through legislation [2]. Plants operating aluminum smelters need to meet hydrogen fluoride emission limits imposed by authorities. Not meeting these requirements could expose the plant to fines or even to reduce or halt the production. Rio Tinto is a responsible company that follows ecological standards to reduce emissions and protect the environment and was the first company to obtain certification by Aluminium Stewardship Initiative (https://aluminium-stewardship.org/). Their modern plants go beyond regulatory requirements. The mean fluoride emissions intensity remains below the world's average of the pre-bake technologies, which is 0.52 kg F_t/t Al [3].

Aluminum smelting operations are commonly complex. The dynamics of HF emissions are affected by a range of factors; increased alumina feeding [4], increased production capacity beyond the GTC gas capture capability, operational deficiencies, poor parameter control, and the gas flow rate [2, 4]. All other process variables being equal, the emission intensity may depend on the HF generation, which depends significantly on the potline current given a specific pot design.

We used advanced numerical simulations to predict HF emissions from roofing vents during specific activities. ANNs can track user activity and build a personalized database to determine patterns for specific activities. To our knowledge, this Rio Tinto plant is the first to use ANNs for modeling HF emissions based on operational and process factors.

2. The Problem Statement and Our Approach

Smelters operate under strict regulatory scrutiny for health and environmental performance [5]. If fluoride emissions exceed limits, it may restrict initiatives like amperage increase. Recent studies and growing demand from smelters have pointed to the need to map the impact of each operation on the fluoride emissions. Instead of just measuring generic emissions, as it was looked at in previous studies [4, 5, 6, 7, 8], a pragmatic approach is now required to take appropriate actions and help companies cut down the emissions intensity from the sources. Pragmatism means the inquiry of the way a specific smelter's operational context contributes to the total HF emission intensity, finding the relationship between the HF emission intensity and individual operations and process factors. Our research explores the predictive multifactorial modelling with artificial neural networks. Using supervised machine learning from multidimensional data sets can allow acknowledging patterns and taking appropriate preventive actions.

Supervised machine learning approach for gaseous HF emissions focuses on learning statistical functions from multidimensional data sets to make generalizable predictions about sources of variance in HF emissions. Such datasets cover electrolytic process, operations, operational excellence, and systemic data. The goal is to provide an understanding of why this approach is relevant for smelters, given its potentiality to increase the problem solving and decision-making capabilities related with the amperage increase and the conformity with regulatory limits.

The next chapter will be devoted to Artificial Neural Networks that were used to model the level of gaseous HF emissions as a function of systemic, structural, process, and operational factors.

3. Method and Procedure

3.1 Data Integrity and Accuracy Requirements

Data Sources:
A supervised machine learning approach for gaseous HF Data needs to be of high quality so that one can make reliable decisions while guaranteeing validity. Multiple data sources were used to gather data. Approximately 91 % of the data used the automated collection approach (e.g., of sensor-derived collection approach); the manual recording of empirical observations comprised only 9 % of the collection method. Automated data recording has an edge in eliminating errors owing to oversight and transcription.

Accuracy Requirements:
Among the most familiar accuracy requirements is the synchronicity based on spatial and temporal components. Data synchronization ensures accuracy and consistency. It reinforces congruence between the effect of the factors measured for each source.

Data Organization:
Data should be organized in a usable form, potentially requiring a conversion/transformation to make it user friendly. Data were checked for homoscedasticity or logarithmic transformation would be addressed otherwise. A more significant issue related with heteroscedasticity is the case that the standard errors could be biased for some independent variables. The only variable that failed the normality test was the metal height; this could be justified because two designs coexisted with different targets. The transformation of this continuous variable to near normality using the Johnson Su distribution helps mitigate the negative effects of outliers or a heavily skewed distribution.

3.2 Data Analysis and The Instrument

3.2.1 Instrument

Neural networks are functions of a set of derived inputs, called hidden nodes that are nonlinear functions of the original inputs. In neural networks, a hidden layer is located between the input and output of the algorithm, in which the function applies weights to the inputs and directs them through an activation function as the output. The functions employed at the nodes of the hidden layers are called activation functions. The activation function is a transformation of a linear combination of the X variables. In this investigation, we used a tangent hyperbolic transformation as an activation function instead of a linear, a polynomial chaos, or a Gaussian function because of its saturation at strongly negative and positive rates of inputs and its sensitivity around zero. A hyperbolic tangent function has some desirable properties: (a) it is antisymmetric, (b) it is asymptotic to -1 and 1, and (c) its slope at 0 is 1. Given a fix intercept, this activation function can mimic the HF generation and emission behavior while adapting to the factors' behavior.

Per the literature, the main attributes of an activation function are to be bounded, parametrizable, often nonlinear, and monotonically expanding [9]. These characteristics are relevant to this application because a process that output emissions will vary in a symmetrical interval around zero when normalized with the intercept. The model uses least absolute deviations instead of least squares; this option was useful to minimize the impact of response outliers.

3.3 Data Sampling Procedures

Eleven continuous variables, including one dependent and 10 independent variables, were chosen for the statistical modeling of the HF generation and emissions. As all variables were pertinent to typical potline operational activities, we determined the covariance using the predictor screening approach. The variables could be classified into four different categories, termed systemic, structural, process setting, and operational excellence categories. Systemic factors cover the distributional function for the workload. Reduction operational excellence consisted of the cell hooding and anode covering efficiency. Structural factors combined different conversions of the initial cell design that affect the gas kinetics. These factors consider the anode geometry, liquid heights, and the gas expansibility space. The process variables comprise the electrolyte temperature and its superheat, the gas temperature, the draft to amperage ratio, the pot internal energy, and the AlF_3 consumption rate. The dependent variable was the measured HF by the CEM at roof vents.

Continuous Sampling:
We followed the continuous sampling procedure to forecast the HF level given the operational activities patterns. Continuous sampling is preferred to the discrete approach because it yields greater informative details of the patterns. The data depth was 4 years and the width covered over 95 % of typical standard activities.

3.4 Choice of the Method

Although the data in the aluminum electrolytic process seems interrelated in the way variables interact, neural circuits address this complexity and by identifying patterns as exhibited in Figure 1. Numerical resolutions of the mathematical equations require accurate knowledge of the system dynamics. However, the complexity of the problem itself, given the number of independent variables, may introduce uncertainties, making the numerical resolution modeling nonrealistic.

Artificial neural networks use algorithms to learn from experience, identify patterns, and improve performance. The potline variables as outlined in Figure 1 are diverse; proper selection of the variables affecting the HF generation and emissions is important for the ANNs to mimic this complex behavior for effective cause identification. But the ANNs require training examples to learn and perform properly.

3.5 Network Design Considerations

Three layers made up the ANNs as showed in Figure 1: inputs, activation-function, and output. The activation function layer comprised three nodes H1_1, H1_2, H1_3 grouping all independent variables; most computation and transformations in the algorithm are introduced here.

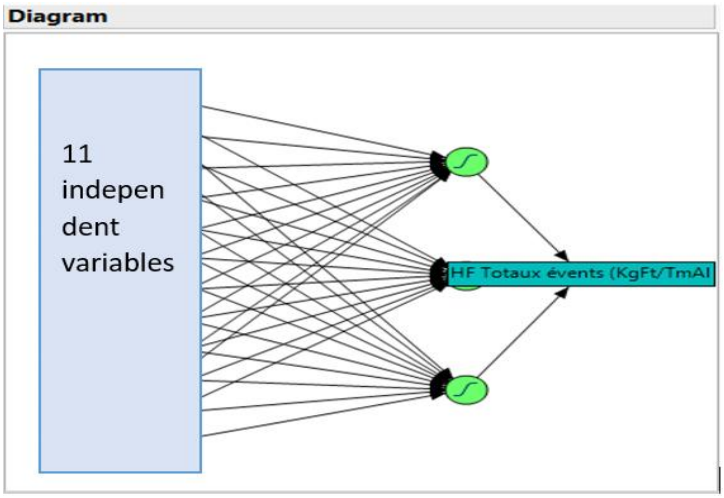

Figure 1. Network design.

4. Results

4.1 Validity

Accuracy (bias) and precision (variability) are two measures of observational errors. While the accuracy is the degree of closeness of measurements to the true value, the precision relates to the reproducibility and repeatability of a measure [4].

4.2 Model Accuracy/Bias

Regarding accuracy, we analyzed the difference between the mean of the predicted values and the reference value from the CEM system. A regression model is proposed in Figure 2, which shows a significant correlation between the two means. The trend line of the accuracy was also plotted to assess the model consistency. Figure 3 shows that accuracy was consistent across the timeframe, close to 93 % throughout the prediction time frame.

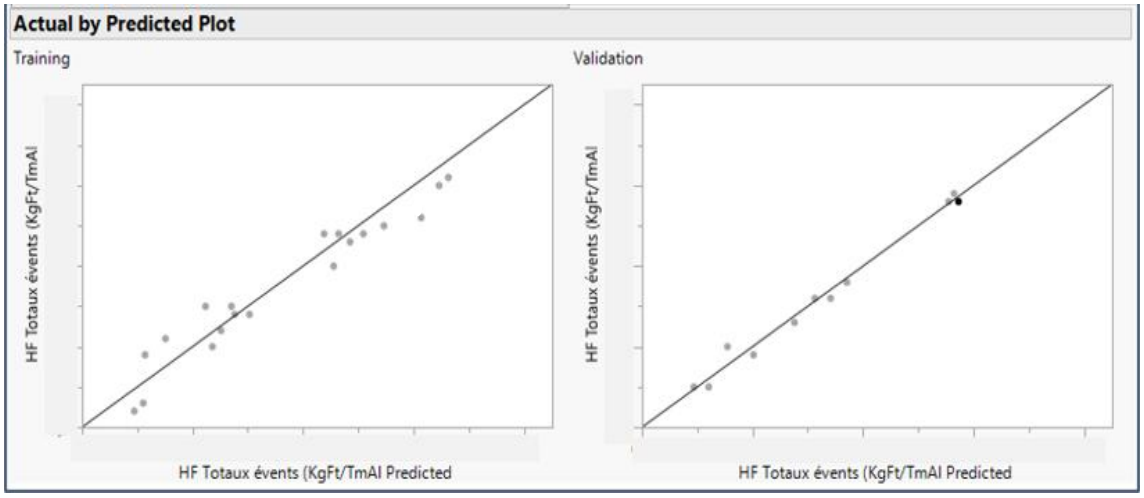

Figure 2. Actual vs predicted correlation.

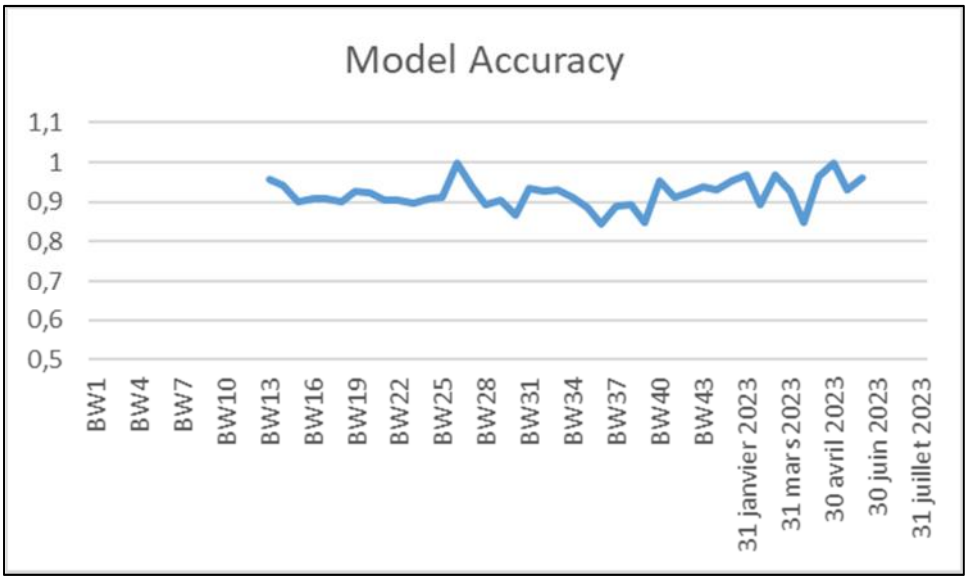

Figure 3. Model accuracy.

4.3 Variability/Precision

Even with constant conditions, the model can still produce different output, which is called variability. Mean precision in this study was estimated at 96 % (*SD = 0.02*), see Figure 4. The lowest precision was recorded at 85 % for two occurrences in a sample size of 34; the maximum was recorded at 100 %.

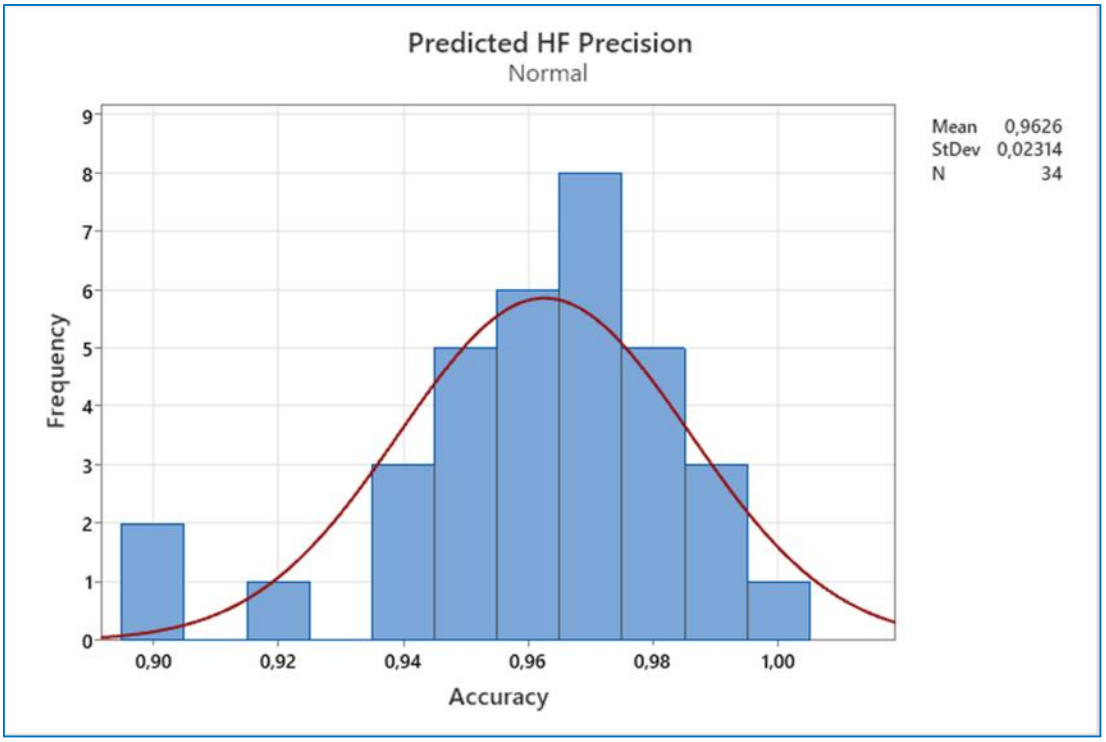

Figure 4. Variability of the prediction.

The quality of the prediction was also assessed based on the main statistical indicator for performance, as illustrated in Figure 12.

The histogram exhibited in Figure 5 displays the predicted values and actual values measured by CEM, verifying their distribution patterns. The data shows a statistically significant equivalence between the two distributions. By comparing the predicted values with actual values measured by CEM, the model for predicting HF gaseous generation and emissions via the ANNs was valid (see Figure 6). It can detect the sources and magnitude of variations for each factor and perhaps help to plan long-term performance.

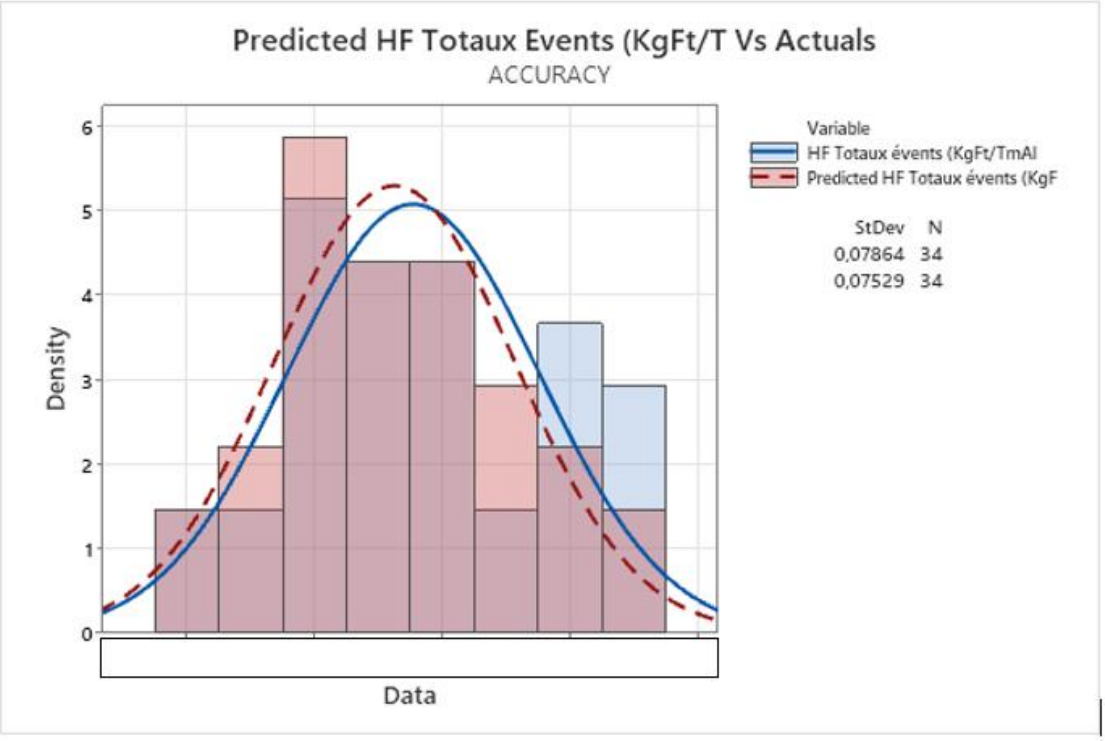

Figure 5. A histogram showing high repeatability and reproducibility.

4.4 Prediction Output Versus CEM Measurements

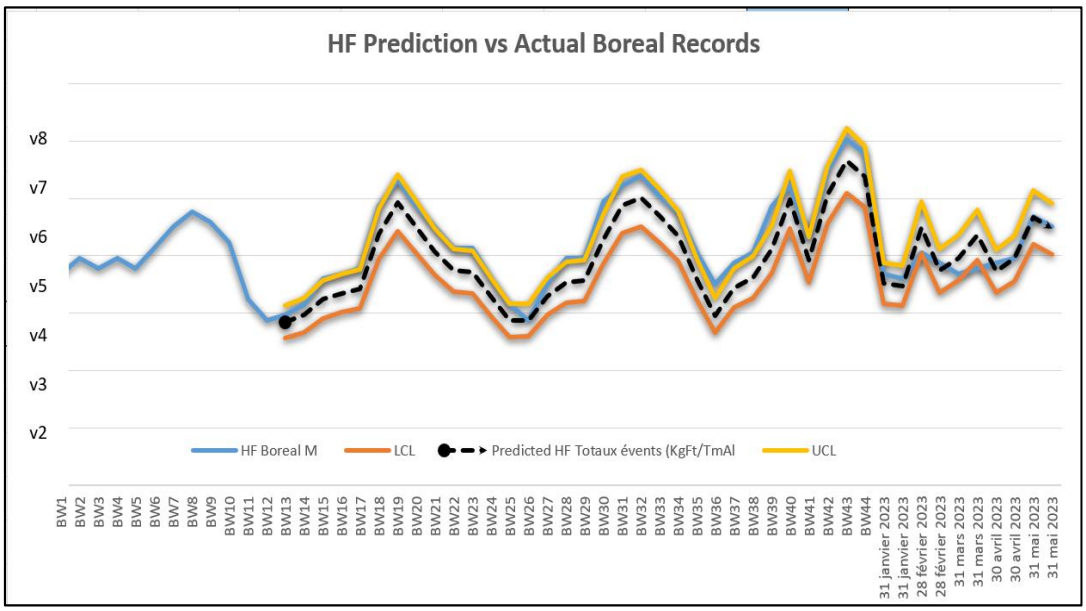

Figure 6. Prediction output Vs CEM.

4.5 Contour Profiler and Response Slider

Contour Profiler exhibits HF response contours for two factors, which are influenced by process settings and operational conditions. Multiple contour plots for different combinations of factors can also be viewed at the same time. Contour profiling was useful for graphically optimizing and visualizing HF generation and emissions.

The doted colored lines on the graph are the contours for the responses set by the Y slider controls or by entering values in the Contour column. One can change the settings for the responses directly from the Contour Profiler report to find the process variables that help meets the setting. The highlighted area shows the domain of the parameter setting for which gaseous HF generation and emissions can exceed pre-determined limits (e.g., 0.5 kg F/t Al).

The quality of the anodes covering can be correlated with the superheat to predict the HF emissions, as illustrated in Figure 7. High electrolyte super heat and huge stress on anode covering can be detrimental to the HF performance. With this software, one can flexibly select a different input variable and appraise the changes in the HF performance. Figure 8 shows the response slider which allows to build an interactive graph automatically.

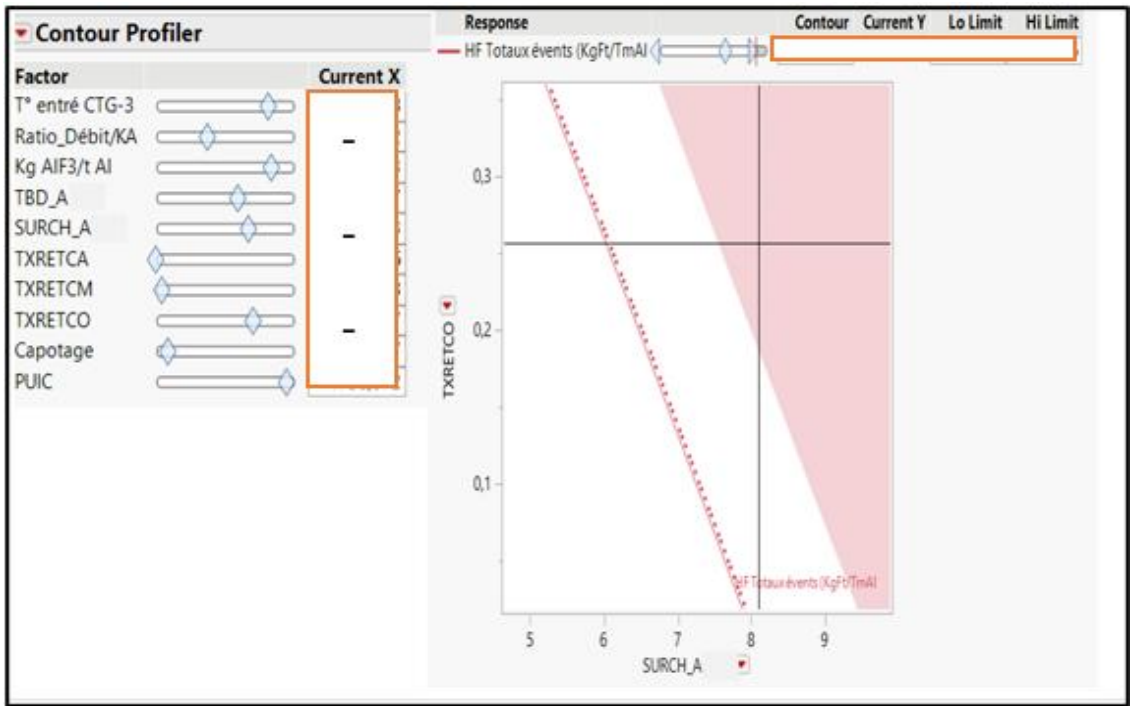

Figure 7. Contour profiler for HF emissions mapping

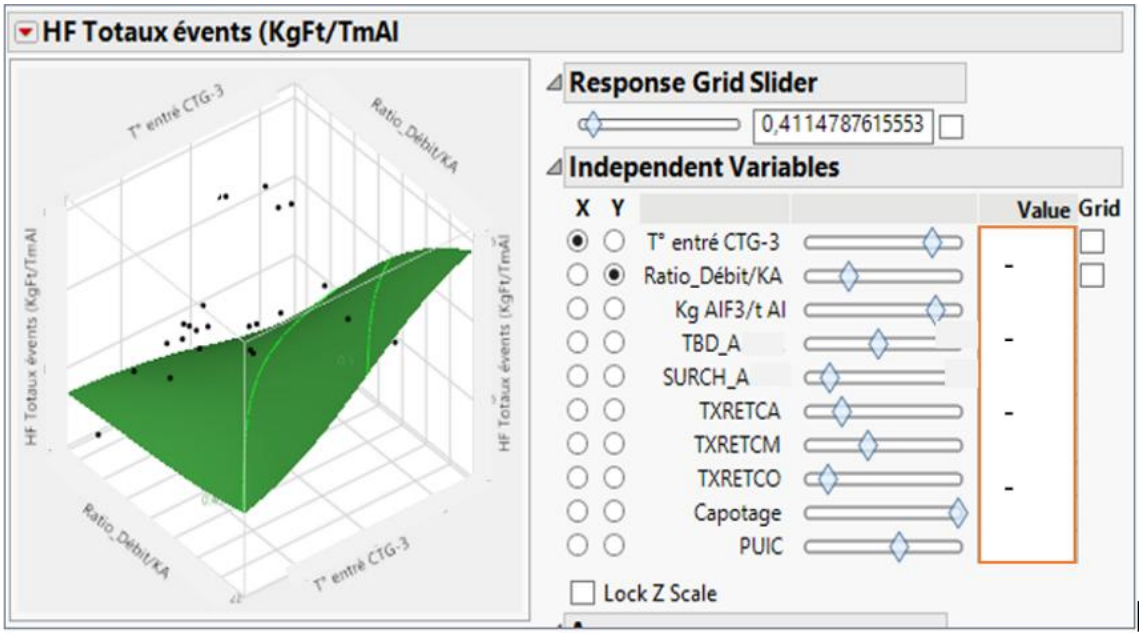

Figure 8. Interactive graphical capability to show the shape.

Any loss of a GTC fan in conditions of high electrolyte temperature and superheat can cause higher HF emissions (Figure 9). We can create various situations for the pot line condition to see how it affects the gaseous HF response. For instance, it can clearly be demonstrated that it is best not to schedule significant maintenance operations during hot summers or high potline temperatures.

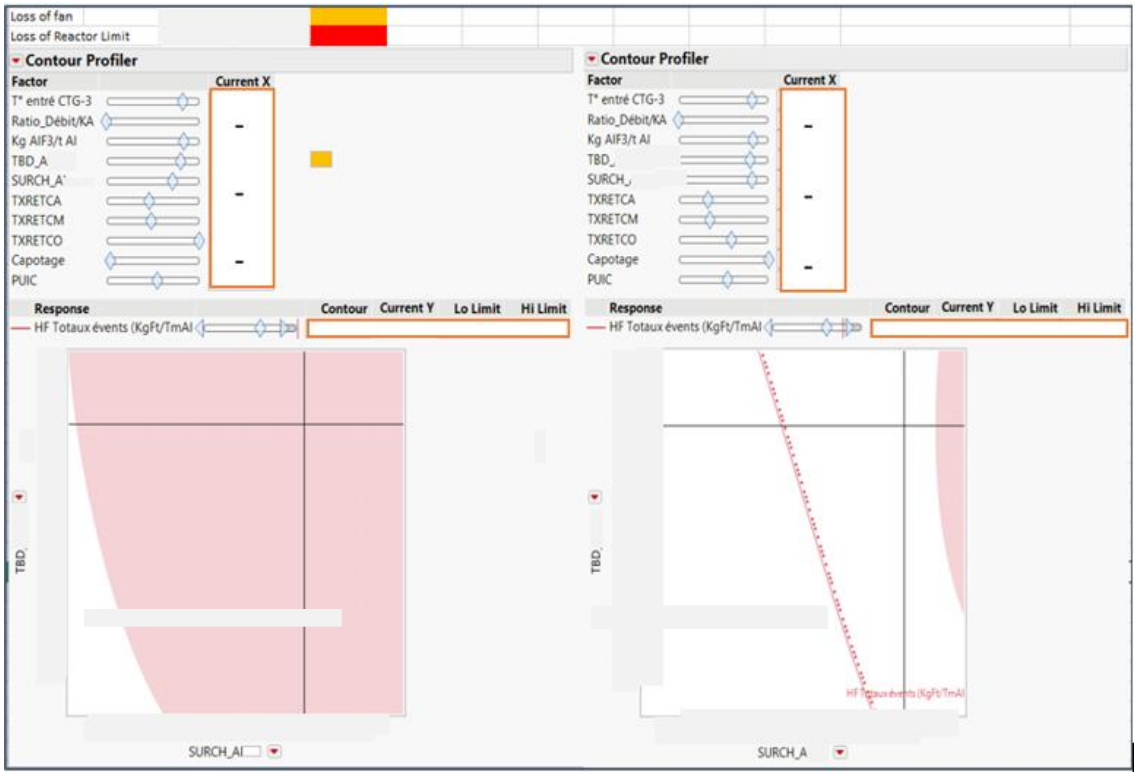

Figure 9. Simulation of a possible loss of a GTC fan.

4.6 Planning Preventive Maintenance in the GTC and HF Emissions

One can predict harsh conditions when we lose a reactor/fan and or perform periodic maintenance in harsh summer conditions. This can be done at scalable current (kA). Sample predictions in varying operating conditions are provided in Figures 10. Figure 11 shows an inverted scenario, where the gas suction rate increases to 404.8 Nm^3/s.

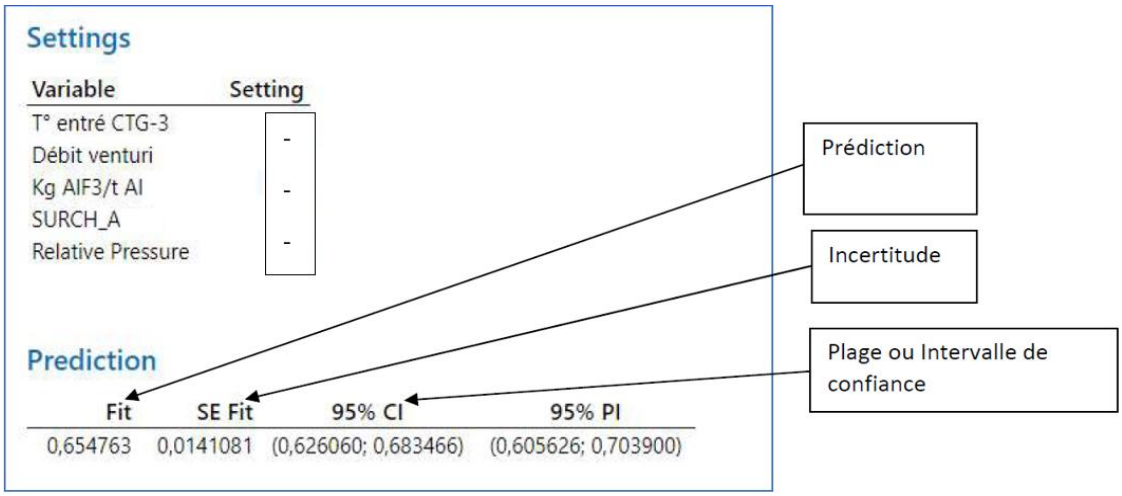

Figure 10. Planning preventive maintenance/emergency situations in the GTC and HF emissions.

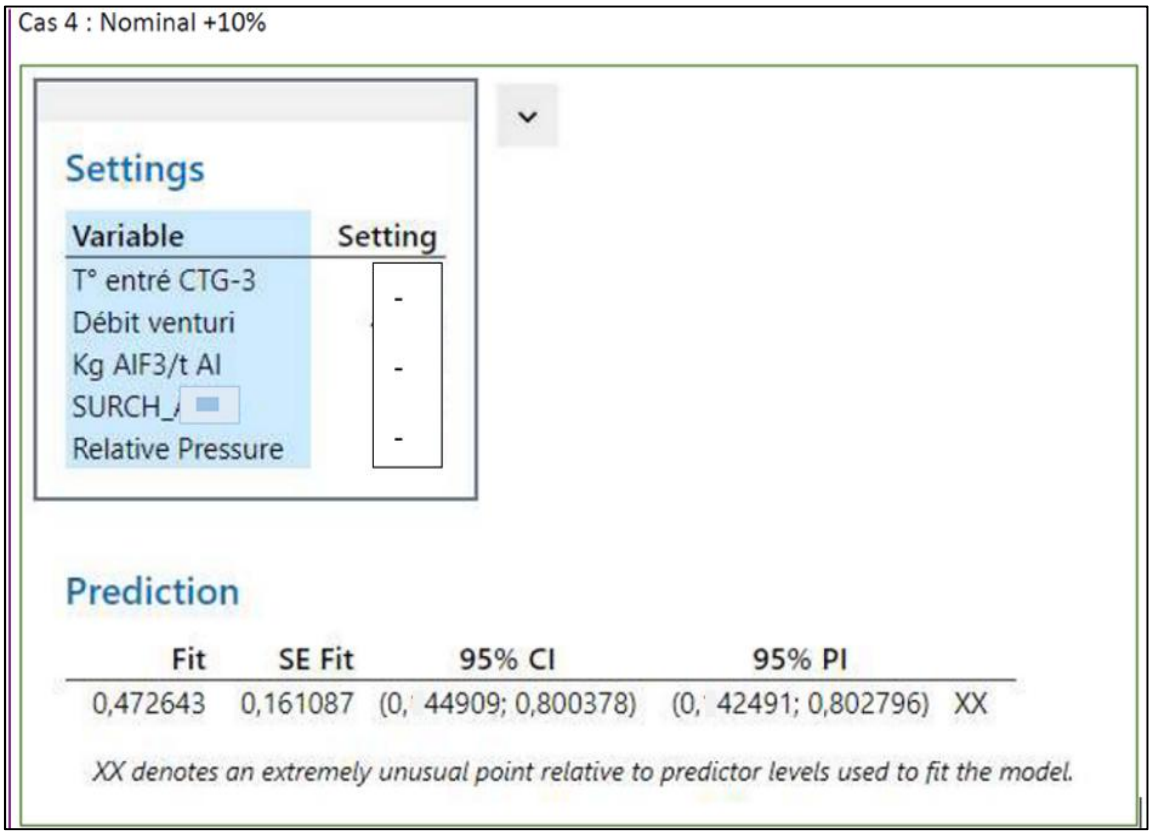

Figure 11. The effect of higher GTC gas flow.

5. Discussion

5.1 ANNs: Algorithms Implication to Business Change

ANN is the statistical knowledge that targets the development of complex computer systems to solve problems by providing the cognitive algorithms for performing tasks that usually exceeds human capability. ANN algorithms are not based on explicit rules as they are adaptive [10]; outputs are generated by multiple data training procedures through sequential computations. This adaption is crucial to a context where multiple predictors interact to yield HF emissions intensity. ANNs use different types of activation functions among which, we selected the non-linear ones because they have huge business applicability in complex data processing. Non-linear functions such as the hyperbolic tangent has showed significant power to process complicated electrolyte process data and mimic HF patterns.

Random error was one of the major model's KPIs to minimise in attempting to achieve consistency. To increase accuracy, a training set of inputs and corresponding target output was given to the algorithm. The weights between the nodes were adjusted for error reduction to attain the desired output. The computer then performed successive iterations during this process until the result converged to the target output (CEM).

Assessing the model stability and consistency involved also comparing its performance during training and validation. Numerous statistics were assessed for, validity, accuracy, and consistency.

- *R-Squared* (square of correlation coefficient) was 0.92 and 0.98 for the training and validation data respectively.
- *RASE* (is a measure of the average error between predicted and actual values) was 0.02 for the training data and 0.0098 for the validation,
- MAD (is the average distance between each data value and the mean, spread of the data in the dataset), was 0.02 and 0.008 for the training and validation data respectively, and
- SSE (the measure of the random error, or the unexplained variation) confirmed the performance of the model; the SSE was minimal (0.017 and 0.001) for the raining and validation respectively.

The model performance is given in Figure 12.

Training		Validation	
HF Totaux évents (KgFt/TmAl		HF Totaux évents (KgFt/TmAl	
Measures	Value	Measures	Value
RSquare	0,922067	RSquare	0,9865323
RASE	0,0285808	RASE	0,0098777
Mean Abs Dev	0,0244546	Mean Abs Dev	0,0082837
-LogLikelihood	-44,85768	-LogLikelihood	-35,18394
SSE	0,0171542	SSE	0,0010733
Sum Freq	21	Sum Freq	11

Figure 1. Model performance.

5.2 Other Practical Learning Benefits

In some practical cases, smelters are forced to enlarge the anode size to lower the current density and the total liquid height to increase heat dissipation. ANNs can predict these changes in HF intensity based on input variability.

We also demonstrated that the rate at which a gas effuses (expressed as the number of molecules passing through the shield opening per second) can be given by the kinetic theory and is proportional to the pressure difference.

$$\Delta P = P_{int} - P_{atm} \quad \text{and} \quad P_{int} = P_{gas} - P_{suct} = P_{(+)} - P_{(-)} \tag{1}$$

where:

P_{atm} Atmospheric pressure outside the hooding.
P_{int} Pressure inside the pot hooding, it is the difference between gas pressure and suction.
P_{gas} Gas pressure = $P_{(+)}$, this pressure is positive
P_{suct} Gas suction at the cell inlet = $P_{(-)}$;

$P_{(+)}$ and the GTC suction $P_{(-)}$ are at the cell inlet, not at the GTC fans.

For a given electrolytic cell, the aspiration force at a pot duct (inlet) is lower than that at the outlet (connected to the fans) of the same duct because of the charge loss. Depending on the conditions (e.g., aging, maintenance quality, anomalous on the piping), the pressure loss can exceed 3-7 % of the nominal values. This loss should be factored when planning to add capacity to the potline considering the GTC capability. ANNs used the suction rate at the cell inlet.

Typically, ΔP should be always < 0 in maintaining effective gas collection at the electrolytic cell level.

A value of $\Delta P > 0$ indicates that significant amount of gas will escape from the pot under-hooding space even in idle situations; and the effusion may deteriorate during activities such as anode setting, shield opening, metal tapping, as well as low anode covering quality.

$P_{int} = P_{gas} - P_{suct}$; Two pressure types are in competition, P_{gas}, which principally depends on the number of particles that increases at scalable pot line amperage. This pressure likewise depends on the available space (e.g., it increases with increasing anode length and increasing liquids height). Figure 13 shows the number of shields that can be opened to still have acceptable gas suction above the break-even point. Thus, smelters must be conscious of small structural changes that, over time, may add up and drive emissions up. Below the break-even, gas entrainment will decrease, and emissions will go up during anode setting, covering, and metal tapping. Air pressure boosters may be added if the maximum capacity falls below critical limits during harsh pot line activities.

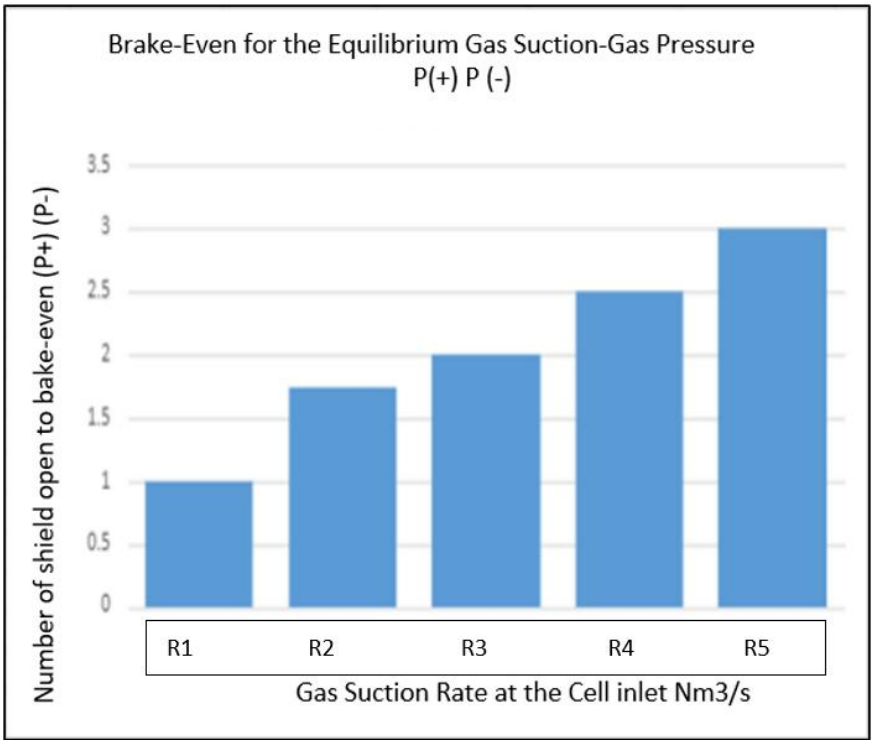

Figure 13. Test of suction effectiveness vs number of shields open.

As the GTC ages and or main components, such as reactors and filters undergo periodic maintenance, P_{suct} would drop gradually, as a result, $P_{int} > P_{atm}$ and $\Delta P > 0$; Any loss of a GTC fan in conditions of high electrolyte temperature and superheat can cause higher HF emissions (Figure 9). It's best not to plan major periodic maintenance in summers and when potline thermal condition is uncertain. High temperatures occur not only during the summer but also when work volume upsurges in the line.

The material accumulated in the basement and on the operating floor may be highly concentrated with HF particulates. HF emissions in the particulate form may surge in summer when this material is churned or agitated for cleaning. Aspiration may be needed rather that churning/tilting where possible.

6. Conclusions and Application to the Business

In the presence of high similarities, confounding factors, or even partial overlaps between operations in the pot line, identification of the causes of high HF emissions is almost out of reach with the current basic linear predictive models and traditional methods of problem-solving. When addressing real electrolysis problems where consistency and accuracy are important in decision-making and planning, the capacity of the neural network systems to mimic complex process behavior for effective problem solving is deemed invaluable. Figures 6 and 12 show that the model accurately predicted the correct HF when compared to CEM and proved the capability of ANN in addressing multifactorial problems.

The output of the ANN model is reliant on the characteristics of the activation function it carries under the hidden nodes. Neural networks achieved over 90 % accuracy in predicting HF generation and emissions during the multifactorial problem-solving. The model can pinpoint factors and calculate their partial contribution to the HF distributional function. Better performance can be achieved by adjusting gas flow, workload, electrolysis settings, and integrating gas kinetics into the amperage increase management. The ANN model allowed to

establish a dashboard that played a key role in monitoring the factors that impact HF emissions and performance.

These arguments conclude the investigation and present smelters with an innovative approach using AI for complex analytics issues. Predictive modeling benefits from ANNs by enabling computers to make smart decisions independently. This is because they can learn and model the relationships between input and output data that are nonlinear and complex. Advanced analytics can be made easier for aluminum smelters by combining this ANN technology with other knowledge in aluminum electrolysis.

7. References

1. El Hani Bouhabila et al., Electrolytic cell gas cooling upstream of treatment center, *Light Metals* 2012, 545-550.
2. *Code of Practice to Reduce Emissions of Fine Particulate Matter (PM2. 5) from the* .https://publications.gc.ca/collections/collection_2016/eccc/En14-241-2015-eng.pdf (retrieved on 30 July 2023).
3. International Aluminium, https://international-aluminium.org/statistics/fluoride-emissions/ .
4. Neil R. Dando and Robert, Fluoride evolution/emission from aluminum smelting pots–impact of ore feeding and cover practices, *Light Metals* 2005, 363-366.
5. Nursiani Tjahyono, Yashuang Gao, David Wong, Wei Zhang, Mark P. Taylor, Fluoride emissions management guide (FEMG) for aluminium smelters, *Light Metals* 2011, 301-306.
6. Karen Sende Osen et al., HF measurements inside an aluminium electrolysis cell, *Light Metals* 2011, 263-268.
7. Y.J. Yang, M. Hyland, Z.W. Wang, & C. Seal, Modelling HF generation in aluminium reduction cell, *Canadian Metallurgical Quarterly*, 54(2), 149-160.
8. Øyvind T. Gustavsen and Terje Østvold, Effect of LiF on the vapour pressure over cryolite containing melts, *Light Metals* 2001, 357-364.
9. Jun Han & Claudio Moraga, The influence of the sigmoid function parameters on the velocity of backpropagation learning, In Mira, José; Sandoval, Francisco (eds.), From Natural to Artificial Neural Computation, Lecture Notes in Computer Science, 1995, Vol. 930, 195–201, https://doi.org/10.1007/3-540-59497-3_175 .
10. L. Ben-Brahim and S. Tadakuma (1998, August). Practical considerations for sensorless induction motor drive system. In IECON'98. Proceedings of the 24th Annual Conference of the IEEE Industrial Electronics Society (Cat. No. 98CH36200) (Vol. 2, 1002-1007). IEEE, https://doi.org/10.1109/IECON.1998.724231 .